

# Oxygen radical inhibition of nitric oxide-dependent vascular function in sickle cell disease

Mutay Aslan<sup>\*†‡§</sup>, Thomas M. Ryan<sup>†§</sup>, Brian Adler<sup>¶||</sup>, Tim M. Townes<sup>†§</sup>, Dale A. Parks<sup>\*\*‡</sup>, J. Anthony Thompson<sup>†\*\*</sup>, Albert Tousson<sup>††</sup>, Mark T. Gladwin<sup>\*\*§§</sup>, Rakesh P. Patel<sup>†¶</sup>, Margaret M. Tarpey<sup>\*\*‡</sup>, Ines Batinic-Haberle<sup>¶¶</sup>, C. Roger White<sup>‡||</sup>, and Bruce A. Freeman<sup>\*†‡§|||</sup>

Departments of <sup>\*</sup>Anesthesiology, <sup>†</sup>Biochemistry and Molecular Genetics, <sup>¶</sup>Pathology, <sup>||</sup>Medicine, and <sup>\*\*</sup>Surgery, <sup>‡</sup>Center for Free Radical Biology, <sup>††</sup>Imaging Facility and <sup>§</sup>Comprehensive Sickle Cell Disease Center, University of Alabama, Birmingham, AL 35233; <sup>††</sup>Critical Care Medicine Department of the Warren G. Magnuson Clinical Center, and <sup>§§</sup>Laboratory of Chemical Biology, National Institute of Diabetes and Digestive and Kidney Diseases, National Institutes of Health, Bethesda, MD 20892; and <sup>¶¶</sup>Department of Biochemistry, Duke University Medical Center, Durham, NC 27710

Edited by Louis J. Ignarro, University of California School of Medicine, Los Angeles, CA, and approved August 9, 2001 (received for review June 11, 2001)

Plasma xanthine oxidase (XO) activity was defined as a source of enhanced vascular superoxide ( $O_2^-$ ) and hydrogen peroxide ( $H_2O_2$ ) production in both sickle cell disease (SCD) patients and knockout-transgenic SCD mice. There was a significant increase in the plasma XO activity of SCD patients that was similarly reflected in the SCD mouse model. Western blot and enzymatic analysis of liver tissue from SCD mice revealed decreased XO content. Hematoxylin and eosin staining of liver tissue of knockout-transgenic SCD mice indicated extensive hepatocellular injury that was accompanied by increased plasma content of the liver enzyme alanine aminotransferase. Immunocytochemical and enzymatic analysis of XO in thoracic aorta and liver tissue of SCD mice showed increased vessel wall and decreased liver XO, with XO concentrated on and in vascular luminal cells. Steady-state rates of vascular  $O_2^-$  production, as indicated by coelenterazine chemiluminescence, were significantly increased, and nitric oxide (NO)-dependent vasorelaxation of aortic ring segments was severely impaired in SCD mice, implying oxidative inactivation of NO. Pretreatment of aortic vessels with the superoxide dismutase mimetic manganese 5,10,15,20-tetrakis(*N*-ethylpyridinium-2-yl)-porphyrin markedly decreased  $O_2^-$  levels and significantly restored acetylcholine-dependent relaxation, whereas catalase had no effect. These data reveal that episodes of intrahepatic hypoxia-reoxygenation associated with SCD can induce the release of XO into the circulation from the liver. This circulating XO can then bind avidly to vessel luminal cells and impair vascular function by creating an oxidative milieu and catalytically consuming NO via  $O_2^-$ -dependent mechanisms.

The  $\beta$ -globin mutation in sickle cell disease (SCD) is manifested by a glutamic acid to valine substitution and, ultimately, vascular dysfunction. Upon deoxygenation, intracellular polymerization of HbS occurs, and sickle erythrocytes acquire altered rheological properties (1). Even though the capillary transit time of red cells is brief in comparison to the kinetics of HbS polymerization, increased blood cell interactions with vascular endothelium will occur as a consequence of altered red cell membrane properties and increased vessel wall adhesiveness. Incompletely described signaling mechanisms also induce an inflammatory-like activation state in vascular endothelium indicated by elevated endothelial expression of Fc receptor and the integrins ICAM-1, VCAM-1, and P-selectin (2–5). There are also increased plasma levels of leukocytes (6), “activated” circulating endothelial cells, proinflammatory cytokines, platelet-activating factor, C-reactive protein, and angiogenic stimuli (7, 8).

The mechanisms underlying regional blood flow deprivation during sickle cell crises, as well as the associated pain with consequent tissue injury, remain poorly understood. If tissue ischemia in SCD patients resulted solely from Hb polymerization and red cell deformation, occlusion of small blood vessels such as terminal arterioles would predominate. Whereas this phenomenon certainly contributes to tissue injury in the liver, lungs, kidney, and spleen, it is not sufficient to explain large vessel vasculopathies. For example,

stroke in SCD patients occurs in large and medium-sized arteries (internal carotid and middle cerebral arteries; refs. 9 and 10). Importantly, the quantity or proportion of sickled or dense red cells in the circulation does not correlate with the incidence of painful episodes or other manifestations of vascular occlusion (11, 12). This implies that much of the morbidity and mortality of SCD is caused by alterations in vascular function that occur secondary to red cell sickling, rather than as a consequence of direct vaso-occlusive actions of sickled red cells.

Multiple features of SCD strongly infer a pathogenic role for impaired NO-dependent vascular regulation. For example, vascular production of NO seems to be chronically activated to maintain vasodilation, as indicated by low baseline blood pressure (13) and decreased plasma arginine levels (14). Also, decreased pressor responses to angiotensin II (15), renal hyperfiltration (16), a tendency for priapism (17), and elevated plasma nitrite and nitrate ( $NO_2^- + NO_3^-$ ) levels occur in SCD (18). During vaso-occlusive crisis, an increased metabolic demand for arginine and an inverse relationship between subjective pain scores and plasma  $NO_2^- + NO_3^-$  levels has been reported (18, 19). Finally, therapeutic benefit has been observed in SCD patients receiving inhaled NO and hydroxyurea, a drug frequently used to treat SCD that not only induces fetal Hb levels in SCD patients but also is metabolized to NO (20, 21).

Another hallmark of SCD, increased tissue rates of production of reactive oxygen species, may also contribute to impaired NO signaling. Compared with HbA red cells, HbS red cells have been reported to generate  $\approx 2$ -fold greater extents of  $O_2^-$ ,  $H_2O_2$ , hydroxyl radical (OH), and lipid oxidation products (LOOH, LOO $\cdot$ ) (22, 23). Also, compartmentalization of redox-active transition metals such as iron has been observed in HbS red cells (23). Finally, mice expressing human  $\beta^S$ -hemoglobin displayed indices of increased lipid oxidation and aromatic hydroxylation reactions and, upon exposure to hypoxia, had  $\approx 10\%$  increase in the conversion of liver and kidney xanthine oxidoreductase to the  $O_2^-$  and  $H_2O_2$ -producing oxidase form (24). Appreciating that NO reacts at diffusion-limited rates with  $O_2^-$  and lipid peroxy radicals (LOO $\cdot$ ) to produce secondary products such as peroxynitrite (ONOO $^-$ ) and nitrated lipids [ $LNO_2$ ,  $L(O)NO_2$ ] (25–27), it is proposed that the impaired vascular function and inflammatory activation of SCD vessels could be a consequence of oxygen radical-dependent consumption of NO and production of secondary reactive species (e.g.,  $H_2O_2$  or ONOO $^-$ ) that can also impair vascular function. In

This paper was submitted directly (Track II) to the PNAS office.

Abbreviations: ACh, acetylcholine; DMNQ, 2,3-dimethoxy-1-naphthoquinone; MnTE-2-PyP, manganese 5,10,15,20-tetrakis(*N*-ethylpyridinium-2-yl)-porphyrin; SCD, sickle cell disease; SOD, superoxide dismutase; XO, xanthine oxidase; XOR, xanthine oxidoreductase.

|||To whom reprint requests should be addressed. E-mail: Bruce.Freeman@ccc.uab.edu.

The publication costs of this article were defrayed in part by page charge payment. This article must therefore be hereby marked “advertisement” in accordance with 18 U.S.C. §1734 solely to indicate this fact.

support of this precept, a combination of clinical and knockout-transgenic SCD mouse studies are reported herein that show increased rates of xanthine oxidase (XO)-dependent vessel wall production of 'NO-inactivating  $O_2^-$  in SCD. The increased rates of vessel wall oxidant production caused impairment of 'NO-dependent vascular relaxation in SCD mouse vessels that were corrected by a catalytic metalloporphyrin superoxide dismutase (SOD) mimetic. Finally, multiple lines of evidence showed that the vessel wall, not red cells, was the primary source of 'NO-consuming free radical species in SCD.

## Materials and Methods

### Erythrocyte Superoxide, Hydrogen Peroxide, and Lipid Hydroperoxide Production.

Blood was collected from healthy HbA adult volunteers and homozygous HbS patients in anticoagulated (EDTA) vacutainers as approved by the Institutional Review Board for Human Use at the University of Alabama at Birmingham. All individuals were evaluated for cytochrome *b<sub>5</sub>* reductase and glucose-6-phosphate dehydrogenase activity, and none were reported deficient. After centrifugation, plasma and buffy coat was discarded, and cells were washed and filtered through a cellulose column (Sigma, type 50 and  $\alpha$  cellulose) to remove neutrophils and platelets. Packed RBCs were diluted to a hematocrit of 2.5% (vol/vol) hemoglobin concentration determined with Drabkin's reagent at 540 nm (28), and rates of  $O_2^-$  release over 2 h were quantified spectrophotometrically by CuZn SOD-inhibitable (100 units  $ml^{-1}$ , equivalent to  $\approx 33 \mu g \text{ ml}^{-1}$  SOD) reduction of cytochrome *c* (50  $\mu M$ ) at 550 nm ( $\epsilon_M = 21 \text{ mM}^{-1}\text{cm}^{-1}$ ). In some experiments,  $O_2^-$  release was measured in cells pretreated with 2,3-dimethoxy-1-naphthoquinone (DMNQ; Oxis, 100  $\mu M$ ), 3-hydroxy-1,2-dimethyl-4-pyridone (Aldrich, 0.5 mM), and 4,4-diisothiocyano-2,2 disulfonic acid stilbene (Sigma, 200  $\mu M$ ). Possible Hb interference in determination of rates of cytochrome *c* reduction was evaluated by performing a singular value decomposition analysis (Matlab, Mathworks, Natick, MA). Intracellular  $H_2O_2$  concentrations were calculated from aminotriazole (AT)-mediated inactivation of catalase activity as described (29). Red cells were incubated with 10 mM AT at 37°C, and intracellular catalase activity was determined at 1-h intervals for 4 h. Catalase activity was measured spectrophotometrically based on the consumption of 10 mM  $H_2O_2$  at 240 nm ( $\epsilon_M = 43.6 \text{ M}^{-1}\text{cm}^{-1}$ ). For determining the extent of membrane lipid oxidation, packed RBCs were lysed in hypotonic phosphate buffer (20 mosM, pH 7.4, 4°C), centrifuged at  $30,000 \times g$  for 20 min, and the supernatant was discarded. Membrane ghosts were washed eight times to minimize Hb contamination and stored at  $-20^\circ C$ . For use as a stimulus of lipid oxidation, ONOO<sup>-</sup> was synthesized as described (25), and its concentration was determined spectrophotometrically at 302 nm ( $\epsilon_M = 1670 \text{ M}^{-1}\text{cm}^{-1}$ ). Lipid hydroperoxide (LOOH) content was measured via *N*-benzoyl leucomethylene blue oxidation and quantitated against a *t*-butyl hydroperoxide standard. Protein concentrations were measured at 595 nm by a modified Bradford assay by using Coomassie Plus reagent with BSA as a standard.

**NO Consumption.** Anaerobic solutions of 1.9 mM 'NO were prepared by equilibrating 'NO gas (Matheson) in argon-saturated deionized water. Contaminating nitrogen dioxide ( $NO_2$ ) or nitrous oxide ( $N_2O$ ) was removed by first passing the NO gas through 5 M NaOH. NO (2.5–15  $\mu M$ ) was added to diluted RBCs (Hb =  $3 \times 10^{-5} \text{ g/ml}^{-1}$ ; 0.5  $\mu M$ ), and rates of 'NO consumption were measured electrochemically (Iso-NO, WPI Instruments, Waltham, MA) under normoxic and hypoxic (20–40 mmHg  $O_2$  tension) conditions in a closed, thermally regulated (37°C) and stirred polarographic cell. Hypoxic conditions were established in the reaction chamber by partially equilibrating buffers with nitrogen gas and quantified by using a Clark model YSI 5300 oxygen electrode (Yellow Springs Instruments).

**XO and Alanine Aminotransferase Analysis.** All animal procedures were reviewed and approved by the Institutional Animal Care and Use Committee at the University of Alabama at Birmingham. Plasma and tissue XO activity was measured by reversed-phase HPLC with electrochemical detection of uric acid as described (30). For biochemical analysis of liver tissue, isolated livers were weighed and homogenized in ice-cold homogenizing buffer (50 mM  $K_2HPO_4/80 \mu M$  leupeptin/2.1 mM Pefabloc SC/1 mM PMSF/1  $\mu g \text{ ml}^{-1}$  aprotinin, pH 7.4). Homogenates were centrifuged ( $40,000 \times g$ , 30 min, 4°C), and supernatants were stored at  $-80^\circ C$ . Plasma alanine aminotransferase activity was measured on an automated spectrofluorometer (Cobas-Fara II, Roche Diagnostic Systems). A rabbit polyclonal antibody against recombinant human xanthine oxidoreductase (XOR) fragment was used (1:1,000 dilution) for immunoblot analysis (32). Horseradish peroxidase-conjugated goat anti-rabbit IgG (1:10,000) was used as a secondary antibody, and immunoreactive proteins were visualized by enhanced chemiluminescence (SuperSignal West Pico Substrate, Pierce).

**Fluorescence Microscopy.** Frozen aortic sections and paraffin-embedded liver sections from C57BL/6J or knockout-transgenic SCD mouse were processed for immunofluorescence. Primary antibody incubations were carried out for 60 min at 25°C by using a rabbit polyclonal antibody against XO (1:50). The secondary antibody was Alexa-594 conjugated goat anti-rabbit (1:100, Molecular Probes). For control studies, the primary anti-XO was preabsorbed with excess (1 unit  $ml^{-1}$ ) bovine XO. Nuclei were counterstained with Hoechst 33258 (20  $\mu g \text{ ml}^{-1}$ , Sigma). Images were acquired through a Leitz Orthoplan microscope and analyzed with IP LAB SPECTRUM software (Scanalytics, Billerica, MA).

**Vessel Relaxation and Superoxide Production.** Isometric tension was measured in aortic segments from mice as described (33). Aortic segments were exposed in some cases to various mediators and inhibitors for 1 h, submaximally contracted with phenylephrine ( $10^{-8}$ – $10^{-7}$  M), and acetylcholine (ACh;  $1 \times 10^{-9}$  to  $3 \times 10^{-6}$  M) was added in a cumulative manner to induce relaxation. Vessel  $O_2^-$  production was monitored in aortic segments by coelenterazine-enhanced chemiluminescence (34) by using an automated microplate luminescence reader (Lumistar Galaxy, BMG Lab Technologies). Previous studies have shown coelenterazine to reflect both tissue  $O_2^-$  and ONOO<sup>-</sup> production, differentiable by selective use of SOD and NO synthase inhibitors (34). Isolated vessels were equilibrated in Hanks' balanced salt solution (HBSS) for 30 min at 37°C, and coelenterazine (10  $\mu M$ , Calbiochem) was added. In some experiments,  $O_2^-$  was measured in vessels that were pretreated with xanthine (50  $\mu M$ , Sigma), allopurinol (100  $\mu M$ , Sigma), CuZn SOD (30 units  $ml^{-1}$ , Oxis), manganese 5,10,15,20-tetrakis(*N*-ethylpyridinium-2-yl)-porphyrin (MnTE-2-PyP; 50  $\mu M$ ), catalase (20 units  $ml^{-1}$ , Worthington), BOF-4272 [sodium-8-(3-methoxy-4-phenylsulfanylphenyl)pyrazolol(1,5 $\alpha$ )-1,3,5-triazine-4-olate-monohydrate] a gift from Otsuka Pharmaceutical, Tokushima, Japan (25  $\mu M$ ), and DMNQ (100  $\mu M$ ). The assay system was calibrated by using 0.1–0.5 mU XO plus 50  $\mu M$  xanthine, generating known rates of  $O_2^-$ -dependent cytochrome *c* reduction.

## Results

**Red Cell Production of Reactive Oxygen Species.** Endogenous rates of  $O_2^-$  release under normoxic (150 mmHg  $O_2$ , pH 7.4) conditions were not significantly different in human HbA ( $1.60 \pm 0.25 \mu mol \text{ gmHb}^{-1}\text{h}^{-1}$ ) vs. homozygous HbS ( $1.84 \pm 0.2 \mu mol \text{ gmHb}^{-1}\text{h}^{-1}$ ) red cells (Fig. 1A). The mean Hb content of HbA and HbS red cell preparations was 0.36 and 0.39 gmHb  $ml^{-1}$  packed cells, respectively. Potential interference of lysed cell-derived Hb in the analysis of cytochrome *c* reduction was ruled out by singular value decomposition analysis, which separated the spectral components of the reaction system and identified the elements contributing to the

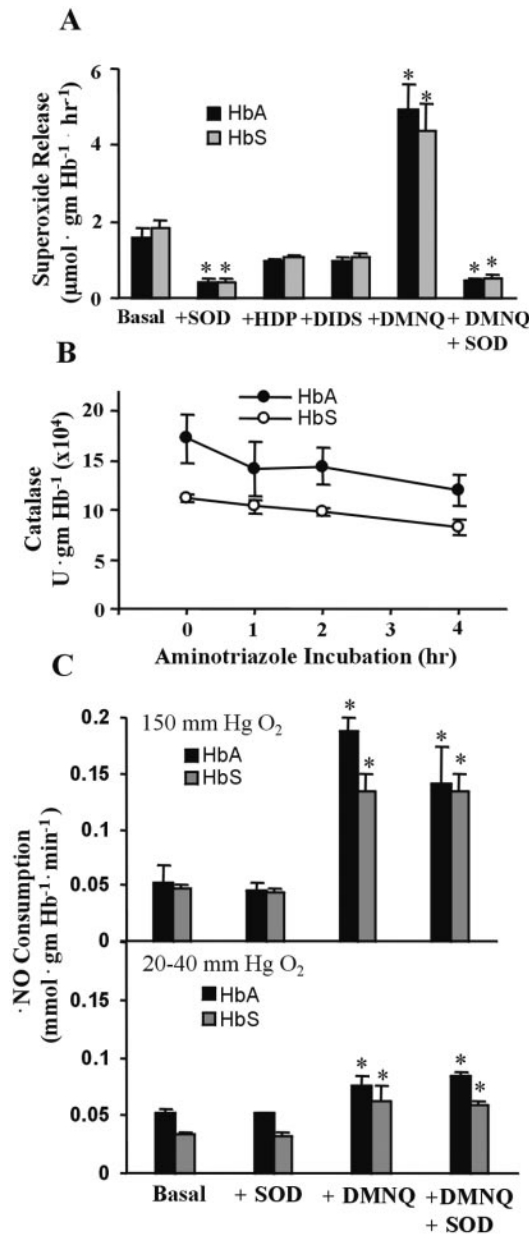


**Fig. 1.** Red cell production of reactive oxygen species. (A) Rates of superoxide release by HbA and HbS red cells. Values are mean ± SEM (*n* = 3–9). Statistical analysis was by two-way ANOVA with the Tukey post hoc test. \*, *P* < 0.05. (B) Aminotriazole-mediated catalase inactivation by HbA and HbS red cells. Values at each time point represent mean ± SD with *n* = 5. (C) Rates of HbA and HbS red cell NO consumption. Values represent mean ± SEM (*n* = 4–14). Statistical analysis was by two-way ANOVA with the Tukey post hoc test. \*, *P* < 0.05 compared with basal.

recorded absorbance. The singular value decomposition analysis of red cell-dependent cytochrome *c* reduction showed a time-dependent increase at 550 nm in the absence of SOD, with only one significant spectral component, reduced cytochrome *c* (not shown). To elucidate the nature of O<sub>2</sub><sup>-</sup> release and verify the specificity of the assay system, DMNQ (100 μM) was added to stimulate red cell O<sub>2</sub><sup>-</sup> production. Preincubation of cells with the metal chelator 3-hydroxy-1,2-dimethyl-4-pyridone (0.5 mM) induced ≈36% decrease in O<sub>2</sub><sup>-</sup>, suggesting that cellular Fe-dependent reactions partially contributed to cell O<sub>2</sub><sup>-</sup> production. When cells were pretreated with a stilbene sulfonate chloride-bicarbonate exchange

**Table 1. Activity of XO and ALT in sickle cell disease**

Measurement	Enzyme activity	
	Control	SCD*
Human		
Plasma XO (μU/ml)	0.89 ± 0.3 (15)	3.30 ± 0.9 (18)
Mouse		
Plasma XO (mU/ml)	2.2 ± 0.26(13)	5.6 ± 1.5 (15)
ALT (mU/ml)	24.2 ± 2.3 (10)	270.5 ± 24.5(12)
Liver XO (mU/g tissue)	53.9 ± 7.8 (6)	18.6 ± 4.4 (6)
Aortic XO (mU/mg protein)	0.29 ± 0.01(3)	0.46 ± 0.03(4)

\*, *P* < 0.05 from control. *n* for each measurement is italicized in parentheses.

protein inhibitor (4,4-diisothiocyano-2,2 disulfonic acid stilbene, 200 μM), both HbA and HbS red cells showed ≈35% decrease in rates of cytochrome *c* reduction, indicating that some extracellular O<sub>2</sub><sup>-</sup> was released through anion channels.

The similar slopes of the time course of aminotriazole-dependent red cell catalase inactivation in HbA and HbS red cells revealed that steady-state H<sub>2</sub>O<sub>2</sub> levels were not significantly different, with calculated H<sub>2</sub>O<sub>2</sub> concentrations of 3.11 ± 2.61 pM and 4.9 ± 2.25 pM, respectively, at 150 mmHg O<sub>2</sub>, pH 7.4 (Fig. 1B). This occurred despite the 36% lower catalase specific activity in HbS red cells, suggesting other compensatory mechanisms for intracellular H<sub>2</sub>O<sub>2</sub> scavenging, e.g., glutathione peroxidase. Accepting that NO reacts at almost diffusion-limited rates with O<sub>2</sub><sup>-</sup> (25), the relative rates of red cell NO consumption was determined as probe for differences in intracellular and extracellular O<sub>2</sub><sup>-</sup> production by HbA and HbS red cells. NO consumption, measured during both normoxic (150 mmHg O<sub>2</sub>) and sickling-inducing hypoxic (20–40 mmHg O<sub>2</sub>) conditions, was not significantly different in HbA vs. HbS red cells, with normoxic values of 0.053 ± 0.016 and 0.047 ± 0.003 mmol gmHb<sup>-1</sup>·min<sup>-1</sup>, respectively (Fig. 1C). Addition of extracellular CuZn SOD (100 units ml<sup>-1</sup>) did not impact the rate of NO consumption, whereas stimulation of cell O<sub>2</sub><sup>-</sup> generation by DMNQ (100 μM) added as a positive control significantly increased rates of red cell NO consumption. The presence of endogenous LOOH was undetectable in both HbA and HbS RBC membranes. When membrane oxidation was stimulated by the addition of OONO<sup>-</sup>, HbS red cell membranes showed greater tendency to undergo lipid peroxidation (not shown).

**Plasma XO and Alanine Aminotransferase Activities.** The catalytic activity of XO was significantly increased in the plasma of SCD patients vs. controls (Table 1). This also occurred in the plasma of a knockout-transgenic mouse model of SCD that synthesizes exclusively human Hb in the murine RBCs (31). The observed increase in plasma XO activity in the knockout-transgenic SCD mouse was accompanied by a decrease in liver XO activity and an increase in plasma alanine aminotransferase activity (Table 1). Western blot analysis of plasma and liver XOR revealed increased plasma and decreased liver XOR protein content in knockout-transgenic SCD mice compared with control or knockout-transgenic sickle cell trait mice, which synthesize both human β<sup>S</sup> and β<sup>A</sup> (Fig. 2A). XOR, which is rapidly converted to the oxidase form (XO) in plasma, revealed immunoreactive 20-kDa, 40-kDa, and 85-kDa proteolytic fragments upon Western blot analysis. Knockout-transgenic sickle cell trait (heterozygous for HbS) mice were also not significantly different from control C57BL/6J mice in plasma and liver XO and plasma alanine aminotransferase activities (not shown). Immunocytochemical localization of XO in aorta and liver (Fig. 2B) of SCD mice showed increased vessel wall and decreased liver XO immunoreactivity, with XO concentrated on and in vascular luminal cells. Hematoxylin and eosin staining of liver of knock-

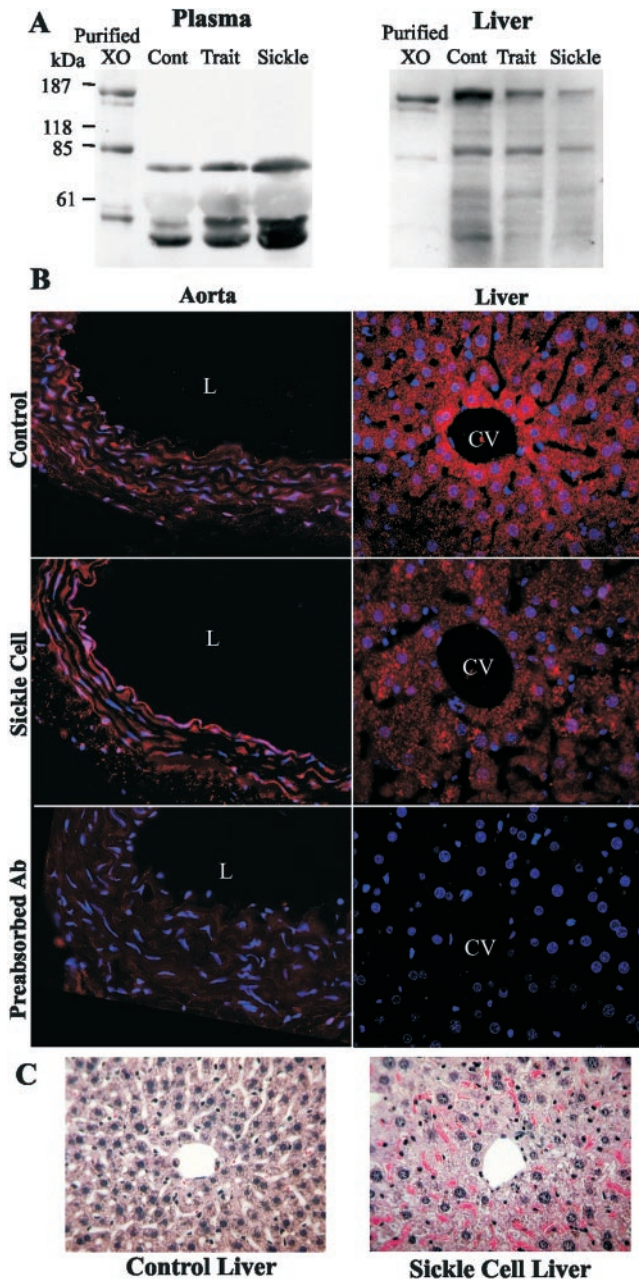


**Fig. 2.** Immunocytochemical analysis of XOR in C57BL/6J control and sickle cell mouse tissues. (A) Western blot analysis of plasma and liver XO in SCD mice. (B) Descending thoracic aortic segments from knockout-transgenic SC mice display intense immunofluorescent staining for XO (red) that is associated with the endothelium and, to a lesser extent, smooth muscle cells (L, lumen). Liver sections from SC mice show decreased XOR staining in the pericentral hepatocytes when compared with controls (CV, central vein). Nuclei were counterstained with Hoechst in all experiments. (C) Hematoxylin and eosin staining of liver sections from control and sickle cell mouse tissues.

out-transgenic SCD mice revealed extensive hepatocellular injury associated with pericentral necrosis. Sickled erythrocytes were also observed in intrahepatic sinusoids (Fig. 2C) (31).

**Superoxide Production and Endothelial-Dependent Relaxation of Vessels.** The catalytic activity of XO was significantly increased in the aorta of SCD mice (Table 1) with a parallel increase in XOR protein observed by Western blot analysis as well (not shown). Basal rates of  $O_2^-$  production were significantly increased in the

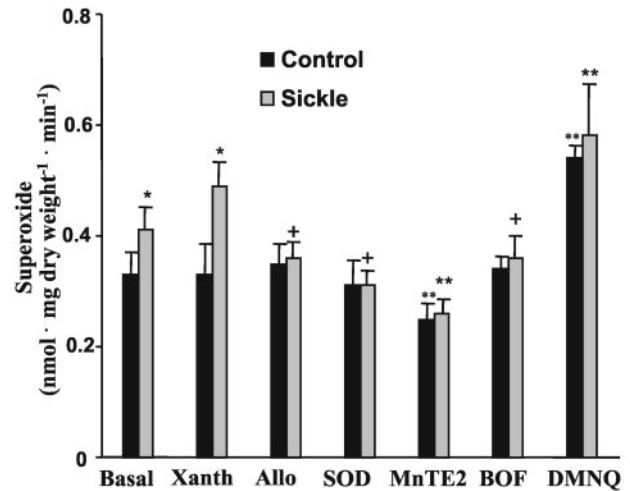


**Fig. 3.** Superoxide production by C57BL/6J control and sickle cell mouse vessels. Values represent mean  $\pm$  SD ( $n = 4$ ). Statistical analysis was by two-way ANOVA with the Duncan's post hoc test. \*,  $P < 0.05$  compared with control. +,  $P < 0.05$  compared with xanthine-treated sickle cell vessels. \*\*,  $P < 0.05$  compared with control and all treated vessel groups.

aorta of SCD mice vs. controls, with rates of  $0.41 \pm 0.04$  and  $0.33 \pm 0.04$  nmol · mg dry weight<sup>-1</sup> · min<sup>-1</sup>, respectively (Fig. 3). In SCD, but not wild-type mouse vessels, rates of  $O_2^-$  production were enhanced by addition of xanthine and returned to basal rates when vessels were pretreated with CuZn SOD (30 units ml<sup>-1</sup>), allopurinol (100  $\mu$ M), or the XO inhibitor BOF-4272 (25  $\mu$ M). Pretreatment of aorta with the SOD mimetic MnTE-2-PyP (50  $\mu$ M) significantly decreased rates of detectable  $O_2^-$  production, whereas DMNQ (100  $\mu$ M) addition significantly enhanced rates of  $O_2^-$  production by both control and SCD mouse vessels. NO-dependent vessel relaxation, elicited by ACh, was severely impaired in SCD mice (Fig. 4). The NO-dependent stimulus of smooth muscle cell guanylate cyclase activity, sodium nitroprusside (100 nM), induced maximal vessel relaxation in SCD mouse

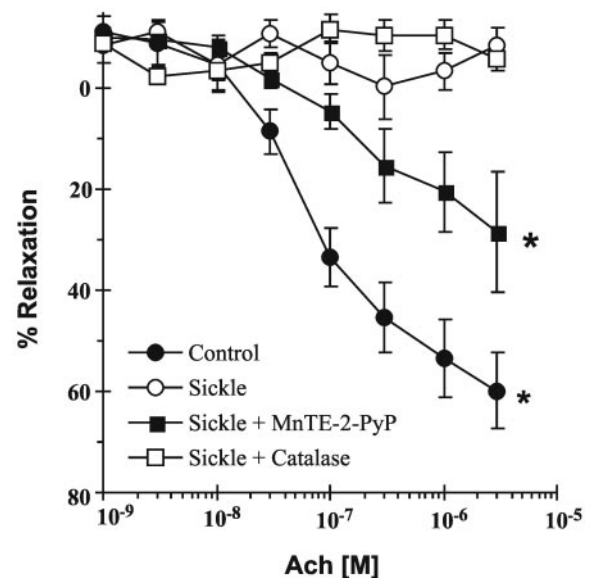


**Fig. 4.** ACh-dependent vascular relaxation in C57BL/6J control and sickle cell mouse vessels. Values represent mean  $\pm$  SEM ( $n = 4-8$ ). All statistical analyses were by one-way ANOVA with Student-Newman Keuls pairwise multiple comparison. \*,  $P < 0.05$  compared with sickle cell mouse vessel response.

vessels, whereas addition of arginine (3 mM) had no effect (not shown). Treatment of SCD mouse vessels with the SOD mimetic MnTE-2-PyP (10  $\mu$ M) significantly restored ACh-dependent relaxation, whereas addition of catalase had no effect (Fig. 4).

## Discussion

Insight into the mechanisms underlying impaired vascular function in SCD is important for guiding the design of more effective therapies to limit vaso-occlusive crisis, acute chest syndrome, stroke, and other circulatory manifestations of this hemoglobinopathy. In contrast to previous reports (22, 23), there is not a significant difference in rates of  $O_2^-$  and  $H_2O_2$  production and basal levels of membrane LOOH content in HbA vs. HbS red cells (Fig. 1A and B). Also, HbA vs. HbS red cells display similar rates of  $^1NO$  consumption under both normoxic and sickling-inducing hypoxic conditions (Fig. 1C). This rules out the possibility that unique oxidative or free radical metabolic properties of HbS red cells contribute to enhanced rates of vascular  $^1NO$  scavenging and in turn initiate pathogenic signal transduction events in SCD vessels, due to suppression of the anti-inflammatory properties of  $^1NO$ . Although the inherent instability of sickle Hb and the possible impairment of tissue free radical defense mechanisms in SCD may render red cells more susceptible to oxidative damage (23, 35), a well-integrated network of oxidant defense mechanisms evidently prevents HbS red cells from becoming significant loci of reactive species production and oxygen radical-dependent inactivation of vascular  $^1NO$  signaling.

The observation that XO activity is elevated in the plasma of SCD patients is recapitulated in the SCD mouse (Table 1), suggesting that this enzyme may serve as a significant source of reactive oxygen species production in SCD. There is only trace XO activity in the plasma and vascular endothelium of healthy humans (36, 37). During pathological conditions such as hepatocellular damage (38, 39), ischemia-reperfusion (40), atherosclerosis (41), adult respiratory distress syndrome (36), alcoholic liver disease (42), and now SCD, in which organs replete in XOR can release this proinflammatory enzyme into the circulation, plasma XO levels increase. This can lead to an enhancement of vascular oxidant production, often in tissue compartments having minimal defense against oxidative injury.

XOR is found mainly in the splanchnic system, where it exists predominantly as a dehydrogenase (XDH/XO; EC 1.1.1.204/1.1.3.22) (43). The hepatic localization of XOR is zonally distributed, with higher activity in pericentral, compared with periportal, hepatocytes (44). The zonal distribution of XOR corresponds to regions where ischemia and hypoxia would be most severe, as oxygen is extracted as blood flows from the portal triad to the central vein branches. During ischemia, XOR can be converted to XO by either proteolytic cleavage of the amino terminus or more rapidly by intramolecular and mixed disulfide formation (45, 46). Significant irreversible proteolytic conversion of cellular XOR to XO is slow, requiring 4–6 h of ischemia (47). However, XOR can be released from ischemic hepatocytes into the circulation before detectable intracellular XOR to XO conversion (48), whereupon either proteolytic cleavage or thiol oxidation may occur rapidly. Repeated interruption of blood flow and the resultant transient ischemia associated with SCD can thus provide the basis for ischemic liver injury and elevated plasma XO levels. During experimental hypoxia, XOR to XO conversion has been shown to be significantly greater in the liver and kidneys of a sickle cell mice model that had a mixture of human HbS and murine Hb (24). In the knockout-transgenic mouse model of SCD used herein, extensive hepatocellular injury (Fig. 2C), accompanied by increased plasma alanine aminotransferase levels (Table 1) and decreased liver XO immunoreactivity (Fig. 2B) and catalytic activity (Table 1), was observed even under normoxic conditions. Even though rodents have much greater XOR-specific activities in plasma than humans (49), release of this enzyme from XOR-replete human

splanchnic tissues can still have potent pathophysiologic effects. Present evidence supports that not only the extent of XO-dependent tissue  $O_2^-$  production, but also its anatomic location, will determine whether or not vascular  $^1NO$ -dependent signaling is adversely affected (50).

The immunohistochemical localization of increased XO in the vessel wall of SCD mice could be a manifestation of either the binding and uptake of circulating XO by vascular endothelial cells (33, 50, 51) or the increased expression of XOR by activated vascular endothelium (52). Considering the high association constant of XO for binding to vascular endothelium ( $K_d = 6$  nM; ref. 53), the presence of XO in the systemic circulation of both SCD mice and humans with SCD implies that a significant deposition of XO can occur in the vessel wall, even when considering the typically low expression of vascular cell XOR in humans (53).

The ability of endothelial-bound XO to remain catalytically active and generate  $O_2^-$  and  $H_2O_2$  at anatomic sites remote from the locus of XO release (50) is consistent with the increased basal rates of  $O_2^-$  production quantified in SCD mouse aorta (Fig. 3). Addition of xanthine enhanced rates of  $O_2^-$  release that were normalized with the XO inhibitors allopurinol and BOF-4272, confirming the XO-mediated increase of vascular  $O_2^-$  and  $H_2O_2$  production in sickle vessels (Fig. 3). The preincubation of control and SCD mouse vessels with CuZn SOD caused a 10% and 32% reduction in rates of detectable  $O_2^-$ , respectively. The modest inhibition of detectable rates of  $O_2^-$  generation by CuZn SOD supports the concept that size exclusion and charge repulsion of this enzyme from the intracellular milieu impedes its ability to scavenge  $O_2^-$  generated by cell-associated XO (50). Pretreatment of aortic vessels with the more cell-avid and membrane-permeable SOD mimetic MnTE-2-PyP (54, 55) had a greater impact on scavenging  $O_2^-$ , giving a 33% and 50% reduction in rates of  $O_2^-$  release in control and sickle vessels, respectively.

XO-derived  $O_2^-$  will react with  $^1NO$  at diffusion-limited rates to impair  $^1NO$  signaling and concomitantly yield secondary oxidizing species, such as ONOO $^-$ , that can further propagate tissue injury (25, 56, 57). A challenge for the future is the delineation of acute versus chronic actions of XO on vascular function in SCD. Although no restorative effects of catalase on vessel relaxation were observed (Fig. 4), XO-derived  $H_2O_2$  can serve as a peroxidase substrate (e.g., for neutrophil myeloperoxidase) that in turn stimulates the catalytic consumption of  $^1NO$  and the formation of secondary oxidizing and nitrating species, possibly leading to more chronic forms of vessel injury (58). A precedent for these phenomena exists in animal models and clinical studies of atherosclerosis. In a hypercholesterolemic rabbit model of atherosclerosis, a 2.5-fold increase in plasma XO severely impairs ACh-mediated relaxation of the thoracic aorta (33, 59). Heparin-induced dissociation of XO from vessel wall binding sites and allopurinol-mediated XO inhibition partially restores ACh-dependent relaxation and decreases vessel  $O_2^-$  production (33). In atherosclerotic and diabetic humans, the XO inhibitors allopurinol and oxypurinol increase forearm blood flow and decrease blood pressure (60, 61). Thus, increased circulating and vessel wall XO in SCD can account for hemodynamic instability and contribute to the pathogenesis of a broader systemic vascular dysfunction. This is exemplified by the observation of impaired  $^1NO$ -dependent vasorelaxation in SCD mice (Fig. 4) and affirms the blunted vascular relaxation that occurs in SCD mouse vessels in response to a calcium ionophore and the  $^1NO$  donor DEA-NONOate (62). This impaired vessel relaxation was restored by denudation of endothelium (62), supporting the presently observed generation of  $^1NO$ -inactivating species by the endothelium of SCD vessels. Importantly, the inhibition of vessel relaxation observed herein was completely restored by sodium nitroprusside (not shown). Because sodium nitroprusside is metabolized by smooth muscle cells (63), this excludes the existence of an end-organ defect in  $^1NO$  signaling and further confirms that  $^1NO$  is being consumed by endothelial-derived free radical reactions in

SCD vessels. This impairment of  $\text{NO}$ -dependent vascular relaxation by increased rates of reactive oxygen species generation was underscored by the observation that the SOD mimetic MnTE-2-PyP restored ACh-dependent relaxation of SCD mouse vessels.

Plasma uric acid and XO levels are strongly predictive of hypertension in normotensive subjects (64). Although hypertension is not associated with SCD, sickle patients with high blood pressure have an increased risk of stroke and death (65). Systolic blood pressure is not increased in an SCD mouse model compared with the background strain (62); however, a 5-fold greater increase in systolic blood pressure is observed in SCD mice when the  $\text{NO}$  synthase inhibitor L-NAME is administered, again affirming the concept of enhanced  $\text{NO}$  consumption and impaired vascular  $\text{NO}$  signaling in SCD.

In summary, episodes of hypoxia-reoxygenation associated with SCD lead to the release of XO into the circulation from

hepatic cells replete in the activity of this source of  $\text{O}_2^-$  and  $\text{H}_2\text{O}_2$ . Increased circulating XO can then bind avidly to vessel luminal cells and impair vascular function by creating an oxidative milieu and catalytically consuming  $\text{NO}$  via diffusion-limited reaction with  $\text{O}_2^-$ . Considering the critical role of endothelial  $\text{NO}$  production in regulating endothelial adhesion molecule expression, platelet aggregation, and both basal and stress-mediated vasodilation, the  $\text{O}_2^-$ -mediated reduction in  $\text{NO}$  bioavailability reported herein can significantly contribute to the vascular disease that is the hallmark of sickle cell anemia.

We appreciate insights and assistance provided by Denyse Thornley-Brown, MD, Elizabeth Lowenthal, MD, Phil Chumley, and Scott Sweeney. This work was supported by National Institutes of Health Grants RO1-HL64937, RO1-HL58115, and P6-HL58418 and by Aeolus, Inc.

- Embury, S. H., Mohandas, N., Paszty, C., Cooper, P. & Cheung, A. T. (1999) *J. Clin. Invest.* **103**, 915–920.
- Belcher, J. D., Marker, P. H., Weber, J. P., Hebbel, R. P. & Vercellotti, G. M. (2000) *Blood* **96**, 2451–2459.
- Hebbel, R. P., Visser, M. R., Goodman, J. L., Jacob, H. S. & Vercellotti, G. M. (1987) *J. Clin. Invest.* **80**, 1503–1506.
- Shiu, Y. T., Udden, M. M. & McIntire, L. V. (2000) *Blood* **95**, 3232–3241.
- Stuart, M. J. & Setty, B. N. (1999) *Blood* **94**, 1555–1560.
- Kaul, D. K. & Hebbel, R. P. (2000) *Clin. Invest.* **106**, 411–420.
- Solovey, A. A., Solovey, A. N., Harkness, J. & Hebbel, R. P. (2001) *Blood* **97**, 1937–1941.
- Solovey, A., Gui, L., Key, N. S. & Hebbel, R. P. (1998) *J. Clin. Invest.* **101**, 1899–1904.
- Stockman, J. A., Nigro, M. A., Mishkin, M. M. & Oski, F. A. (1972) *N. Engl. J. Med.* **287**, 846–849.
- Merkel, K. H., Ginsberg, P. L., Parker, J. C., Jr. & Post, M. J. (1978) *Stroke* **9**, 45–52.
- Ballas, S. K., Lerner, J., Smith, E. D., Surrey, S., Schwartz, E. & Rappaport, E. F. (1988) *Blood* **72**, 1216–1223.
- Lande, W. M., Andrews, D. L., Clark, M. R., Braham, N. V., Black, D. M., Embury, S. H. & Mentzer, W. C. (1988) *Blood* **72**, 2056–2059.
- Johnson, C. S. & Giorgio, A. J. (1981) *Arch. Intern. Med.* **141**, 891–893.
- Enwonwu, C. O. (1989) *Med. Sci. Res.* **17**, 997–998.
- Hatch, F. E., Crowe, L. R., Miles, D. E., Young, J. P. & Portner, M. E. (1989) *Am. J. Hypertens.* **2**, 2–8.
- Allon, M. (1990) *Arch. Intern. Med.* **150**, 501–504.
- Mantadakis, E., Cavender, J. D., Rogers, Z. R., Ewalt, D. H. & Buchanan, G. R. (1999) *J. Pediatr. Hematol. Oncol.* **21**, 518–522.
- Rees, D. C., Cervi, P., Grimwade, D., O'Driscoll, A., Hamilton, M., Parker, N. E. & Porter, J. B. (1995) *Br. J. Haematol.* **91**, 834–837.
- Morris, C. R., Kuypers, F. A., Larkin, S., Sweeters, N., Simon, J., Vichinsky, E. P. & Styles, L. A. (2000) *Br. J. Haematol.* **111**, 498–500.
- Atz, A. M. & Wessel, D. L. (1997) *Anesthesiology* **87**, 988–990.
- Glover, R. E., Ivy, E. D., Orringer, E. P., Maeda, H. & Mason, R. P. (1999) *Mol. Pharmacol.* **55**, 1006–1010.
- Hebbel, R. P., Eaton, J. W., Balasingam, M. & Steinberg, M. H. (1982) *J. Clin. Invest.* **70**, 1253–1259.
- Kuross, S. A. & Hebbel, R. P. (1988) *Blood* **72**, 1278–1285.
- Osarogiabon, U. R., Choong, S., Belcher, J. D., Vercellotti, G. M., Paller, M. S. & Hebbel, R. P. (2000) *Blood* **1**, 314–320.
- Beckman, J. S., Beckman, T. W., Chan, J., Marshall, P. S. & Freeman, B. A. (1990) *Proc. Natl. Acad. Sci. USA* **87**, 1620–1624.
- Radi, R., Beckman, J. S., Bush, K. M. & Freeman, B. A. (1991) *Arch. Biochem. Biophys.* **228**, 481–487.
- Rubbo, H., Radi, R., Trujillo, M., Telleri, R., Kalyanaraman, B., Barnes, S., Kirk, M. & Freeman, B. A. (1994) *J. Biol. Chem.* **269**, 26066–26075.
- Beutler, E. R., ed. (1984) *Cell Metabolism: A Manual of Biochemical Methods* (Grune & Stratton, Orlando, FL), 3rd Ed., pp. 8–13.
- Royall, J. A., Gwin, P. D., Parks, D. A. & Freeman, B. A. (1992) *Arch. Biochem. Biophys.* **294**, 686–694.
- Tan, S., Radi, R., Gaudier, F., Evans, R. A., Rivera, A., Kirk, K. A. & Parks, D. A. (1993) *Pediatr. Res.* **34**, 303–307.
- Ryan, T. M., Ciavatta, D. J. & Townes, T. M. (1997) *Science* **278**, 873–876.
- Parks, D. (1998) in *Reactive Oxygen Species in Biological Systems*, eds. Gilbert, D. L. & Colton, C. (Plenum, New York), pp. 397–420.
- White, R. C., Darley-Usmar, V., Berrington, R. W., McAdams, M., Gore, Z. J., Thomson, A. J., Parks, A. D., Tarpey, M. M. & Freeman, B. A. (1996) *Proc. Natl. Acad. Sci. USA* **93**, 8745–8749.
- Tarpey, M. M., White, C. R., Suarez, E., Richardson, G., Radi, R. & Freeman, B. A. (1999) *Circ. Res.* **84**, 1203–1211.
- Aslan, M., Thornley-Brown, D. & Freeman, B. A. (2000) *Ann. N.Y. Acad. Sci.* **899**, 375–391.
- Grum, C. M., Ragsdale, R. A., Ketai, L. H. & Simon, R. H. (1987) *J. Crit. Care* **2**, 22–26.
- Giler, S., Sperling, O., Brosh, S., Urca, I. & De Vries, A. (1975) *Clin. Chim. Acta* **63**, 37–40.
- Giler, S., Sperling, O., Brosh, S., Urca, I. & De Vries, A. (1975) *Isr. J. Med. Sci.* **11**, 1225.
- Wolko, K. & Krawczynski, J. (1974) *Mater. Med. Pol.* **6**, 95–98.
- Parks, D. A. & Granger, D. N. (1983) *Am. J. Physiol.* **245**, G285–G289.
- Mohacsi, A., Kozlovsky, B., Kiss, I., Seres, I. & Fulop, T., Jr. (1996) *Biochim. Biophys. Acta* **1316**, 210–216.
- Parks, D. A., Skinner, K. A., Skinner, H. B. & Tan, S. (1998) *Pathophysiology* **5**, 49–66.
- Kooij, A., Schijns, M., Frederiks, W. M., Van Noorden, C. J. & James, J. (1992) *Virchows Arch. B Cell. Pathol. Incl. Mol. Pathol.* **63**, 17–23.
- Kooij, A. (1994) *Histochem. J.* **26**, 889–915.
- Enroth, C., Eger, B. T., Okamoto, K., Nishino, T., Nishino, T. & Pai, E. F. (2000) *Proc. Natl. Acad. Sci. USA* **97**, 10723–10728.
- Amaya, Y., Yamazaki, K., Sato, M., Noda, K. & Nishino, T. (1990) *J. Biol. Chem.* **265**, 14170–14175.
- Engerson, T. D., McKelvey, T. G., Rhyne, D. B., Boggio, E. B., Snyder, S. J. & Jones, H. P. (1987) *J. Clin. Invest.* **6**, 1564–1570.
- Yokoyama, Y., Beckman, J. S., Beckman, T. K., Wheat, J. K., Cash, T. G., Freeman, B. A. & Parks, D. A. (1990) *Am. J. Physiol.* **258**, G564–G570.
- Al-Khalidi, A. S. & Chaglassian, T. H. (1965) *Biochem. J.* **97**, 318–320.
- Houston, M., Estevez, A., Chumley, P., Aslan, M., Marklund, S., Parks, D. A. & Freeman, B. (1999) *J. Biol. Chem.* **274**, 4985–4994.
- Radi, R., Rubbo, H., Bush, K. & Freeman, B. A. (1997) *Arch. Biochem. Biophys.* **339**, 125–135.
- Dupont, G. P., Huecksteadt, T. P., Marshall, B. C., Ryan, U. S., Michael, J. R. & Hoidal, J. R. (1992) *J. Clin. Invest.* **1**, 197–202.
- Paler-Martinez, A., Panus, P. C., Chumley, P. H., Ryan, U., Hardy, M. M. & Freeman, B. A. (1994) *Arch. Biochem. Biophys.* **311**, 79–85.
- Patel, M. & Day, B. J. (1999) *Trends Pharmacol. Sci.* **9**, 359–364.
- Spasojevic, I., Batinic-Haberle, I. & Fridovich, I. (2000) *Nitric Oxide* **5**, 526–533.
- Kissner, R., Nauser, T., Bugnon, P., Lye, P. G. & Koppenol, W. H. (1997) *Chem. Res. Toxicol.* **10**, 1285–1292.
- Villa, L. M., Salas, E., Darley-Usmar, V. M., Radomski, M. W. & Moncada, S. (1994) *Proc. Natl. Acad. Sci. USA* **91**, 12383–12387.
- van der Vliet, A., Eiserich, J. P., Halliwell, B. & Cross, C. E. (1997) *J. Biol. Chem.* **272**, 7617–7625.
- White, C. R., Brock, T. A., Chang, L. Y., Crapo, J., Briscoe, P., Ku, D., Bradley, W. A., Gianturco, S. H., Gore, J., Freeman, B. A. & Tarpey, M. M. (1994) *Proc. Natl. Acad. Sci. USA* **91**, 1044–1048.
- Cardillo, C., Kilcoyne, C. M., Cannon, R. O., III, Quyyumi, A. A. & Panza, J. A. (1997) *Hypertension* **30**, 57–63.
- Butler, R., Morris, A. D., Belch, J. J., Hill, A. & Struthers, A. D. (2000) *Hypertension* **35**, 746–751.
- Nath, K. A., Shah, V., Haggard, J. J., Croatt, A. J., Smith, L. A., Hebbel, R. P. & Katusic, Z. S. (2000) *Am. J. Physiol.* **279**, R1949–R1955.
- Kowaluk, E. A., Seth, P. & Fung, H. L. (1992) *J. Pharmacol. Exp. Ther.* **262**, 916–922.
- Newaz, M. A., Adeeb, N. N., Muslim, N., Razak, T. A. & Htut, N. N. (1996) *Clin. Exp. Hypertens.* **8**, 1035–1050.
- Pegelow, C. H., Colangelo, L., Steinberg, M., Wright, E. C., Smith, J., Phillips, G. & Vichinsky, E. (1997) *Am. J. Med.* **2**, 171–177.